# Cryopurification and microbial fuel cell process as a combined approach to treat mine-impacted water

**Ethan Allen**
Western University Faculty of Engineering
**Daria Popugaeva**
Western University Faculty of Engineering
**Carlos Munoz-Cupa**
Western University Faculty of Engineering
**Amarjeet S Bassi**
Western University Faculty of Engineering
**Konstantin Kreyman**
Western University Faculty of Engineering
**Ajay K Ray** ( aray@eng.uwo.ca )
Western University Faculty of Engineering https://orcid.org/0000-0003-4814-6482

**Research Article**

**Keywords:** northern regions, zinc removal, freezing technology, MFC

**Posted Date:** January 29th, 2024

**DOI:** https://doi.org/10.21203/rs.3.rs-3617060/v1

# Abstract

In the current study, a water treatment approach integrating freezing technology, so-called cryopurification, and microbial fuel cell (MFC) process is proposed and tested towards zinc removal. Contaminated water samples used for laboratory experiments were received from the Faro Mine site, Yukon, Canada. Through cryopurification, the effect of freezing temperature, mixing and the direction of ice front propagation on zinc removal from the Faro mine water was investigated and quantitively analyzed. The MFC was used to treat a post-cryopurification brine, both at a laboratory scale. When the coolant temperature ranged from − 5 to − 1$^{\circ}C$ and 180 *rpm* solution mixing was used, up to 80–95% of zinc was removed after a single freezing cycle. The results of laboratory experiments demonstrated that zinc concentrations in mine water can be reduced by cryopurification to 0.5 *mg/L* (effluent quality standard) under optimal experimental conditions. The MFC process was run for 120 *h* to test the capacity of the microorganism (*Shewanella oneidensis*) towards zinc removal from the brine concentrated by freezing. Based on the results of laboratory experiments, MFC showed a reliable and high zinc removal up to 90–93*%* with *Shewanella oneidensis* incubated in the anode. The MFC generated a power density and open-circuit voltage with a maximum result of 8.8 $mW/m^2$ and 168.5 *mV*, respectively.


# Introduction

Freeze concentration, a nature-inspired water treatment technology, also referred to as freeze desalination or cryopurification, is a promising technology for treating contaminated water (Yin et al. 2017; Najim 2022). The process relies on the principle that the structure of ice crystal does not accommodate impurities/salts meaning that they are rejected by the growing ice as water freezes (Shonet 1987). The ice produced through cryopurification is separated from the concentrated solution and then melted to obtain pure water (Najim 2022). The application of cryopurification has several benefits over other common contaminated water treatment and desalination methods (Najim and Krishnan 2023). The energy consumption comparison between cryopurification and conventional evaporative technology showed that cryopurification is energetically more favourable by about 70%, which can be even higher in northern climates. For industrial applications of cryopurification at or near the polar regions, a natural weather advantage is in effect (Najim and Krishnan 2022; Xu et al. 2022; Najim 2022). Most importantly, little to no chemicals are involved in the process of water treatment by freezing and the cost is 2–10 times lower than other methods such as reverse osmosis, evaporative methods, nanofiltration, and distillation according to available literature data (Youssef et al. 2014; Xu et al. 2022).

It was reported based on laboratory tests and field data that freezing technology Is capable of effectively removing several impurities from wastewater and mine-impacted water including metals and heavy metals, such as nickel, cobalt, manganese, chromium, and others (Hasan and Louhi-Kultanen 2016; Melak et al. 2016; Wijewardena 2018; Popugaeva et al. 2021, 2023; Tongshuai et al. 2022). Among cryopurification cons there is a concentrated solution (brine), a by-product of the cryopurification process, that could harm the environment due to its high contaminant concentration. As an alternative to brine disposal, brine treatment promotes the reduction of pollution, minimization of waste volume, and

production of freshwater with high recovery rates. Cryopurification could be combined with other water purification methods, for example, with membrane distillation. Such hybridization (integration of cryopurification with other water treatment methods) has the potential to make cryopurification more beneficial compared to the separate design. In addition, the process can also be integrated with biochemical processes such as microbial fuel cell (MFC). MFC is a process that uses bio-electrochemical processes for voltage generation and shows a potential for heavy metal remediation. The system uses organic substrates and the microorganism's catalytic activity to generate electricity (Dutta and Kundu 2018). Single-chamber and dual-chamber MFCs are the main configurations of MFCs. The first one is also known as air cathode MFC and is composed of one chamber for microbial degradation and one cathode exposed to air. The second type has two chambers, the anode processes the organic matter, and the cathode is exposed to catholyte solutions such as potassium ferricyanide, and they are separated by a proton exchange membrane (Logan 2008; Munoz-Cupa et al. 2021; Obileke et al. 2021). Single-chamber MFC is a configuration that has been utilized for cadmium, chromium, zinc, and copper removal from mining wastewater. (Abourached et al. 2014; Wang et al. 2016; Peng et al. 2017; Vélez-Pérez et al. 2020; Xie et al. 2020). Moreover, dual-chamber MFC has been used for recovery of cadmium, copper, and vanadium (Aiyer 2020), also, zinc was treated in the cathode chamber (Fradler et al. 2014). Additionally, inorganic sulfur compounds in mining wastewater have been investigated for electricity generation using MFC technology (Sulonen et al. 2014; Ni et al. 2016). Furthermore, mining wastewater has been treated by dual-chamber MFC using catholyte reduction in the cathode chamber with different mixtures of microbial cultures in the anode chamber (Ai et al. 2020; Alexandre et al. 2022). However, these processes emphasize in the treatment of organic and sulfur compounds in the wastewater from the mining industry.

In addition, bacterial cultures for metal remediation have been found in the Yukon Territory. Some of these micro-organisms are anaerobic that interact in the metal fixation in soils from Zn-Pb deposits (Gadd et al. 2017; Nielsen et al. 2019). The main cultures used and found in the northern territories are composed of sulfate reduction bacteria. These types of bacteria are composed of different cultures such as *Acidithiobacillus ferrooxidans*, *Pseudomonas putida*, *Bacillus subtilis*, and *Desulfovibrio desulfuricans* that can be used for the removal of different metals such as iron and chromium (Dixit et al. 2015; Makhalanyane et al. 2016). Other microorganisms with metal reduction characteristics have been investigated such as *Geobacter* and *Shewanella oneidensis* is a gram-negative bacterium, that uses extra cellular electron transport (EET) for metal removal and bioelectrochemical processes such as MFC. Additionally, S. oneidensis is a facultative bacterium that can grow under aerobic and anaerobic conditions. This characteristic facilitates the application of the bacterium with different environmental conditions (Min et al. 2017; Yin et al. 2022).

In this work, Faro Mine's water was used as a feed solution to test a novel approach of mine-impacted water treatment: cryopurification in combination with the MFC process towards zinc removal. With a critical analysis of studies performed before, the green water treatment approach could offer significant advantages over conventional treatment approaches including energy efficiency, no chemical pre-treatment, and zero waste generation (i.e. brine). Notably, this approach could be especially beneficial in northern climates due to natural cold temperature conditions promoting cryopurification. The Faro Mine's

water has elevated zinc concentrations that are up to almost 25–30 times above the effluent quality standard of 0.5 *mg/L* (The Government of Canada 2022). Taking this into the account, the objectives of this research work are: (i) to remove zinc from the Faro Mine water in a set of laboratory experiments on cryopurification below or close to the effluent quality standard and (ii) to eliminate the waste product of cryopurification experiments (i.e. brine) by treating brine solution using the MFC process. It is anticipated that this approach could be a sustainable water treatment solution at the Faro Mine site or other mine or industrial sites in Canada's North.

## Materials and Methods

# Study Area

The feed water used for the laboratory experiments was received from Faro Mine site (Fig. 1). The Faro Mine is a legacy abandoned mine located in south-central Yukon (62.3527° N, 133.4054° W), near the town of Faro. The site is located on the traditional territory of the Kaska Nations, upstream from Selkirk First Nation (Crown-Indigenous Relations and Northern Affairs Canada 2021). The physicochemical properties of the mine-impacted water are shown in Table 1. The water has circum-neutral pH and is characterized by elevated zinc concentrations that are up to almost 25–30 times above the effluent quality standard of 0.5 *mg/L* (The Government of Canada 2022; Popugaeva et al. 2023). This is one of the primary concerns for limiting the impact on sensitive receiving environments in the study area.

Table 1
The characteristics of Faro Mine's water

| Parameters | Units | Value |
|---|---|---|
| Zinc (total) | *mg/L* | 13.7 |
| pH | N/A | 7.2 |
| Salinity | *ppt* | 0.9 |
| Total dissolved solids (TDS) | *g/L* | 1.2 |
| N/A – not applicable | | |

# Proposed and tested water treatment approach for zinc removal

In this study, cryopurification was merged with the MFC process for the first time to investigate its joint treatment effect on zinc removal from the mine-impacted water. Figure 2 illustrates the schematic design of the proposed hybrid approach that was a foundation for the laboratory setup containing two main blocks. First one includes the equipment facilitating a cryopurification process of mine-impacted water. The main goal of a second block (MFC) was the treatment of brine solution produced by cryopurification experiments. The feed water was firstly treated by cryopurification and purified water was produced from

the melted ice. Subsequently, the brine produced through cryopurification was sent to the anode of the dual-chamber MFC, after 120 *h* of processing time the bacterium was separated from anode solution with the brine by centrifugation.

For cryopurification experiments, a circulating chiller (bath work area dimensions 16.8 x 17.8 x 15.2 *cm*) was filled with ethylene glycol/water fluid (Cole-Parmer, Vernon Hills, Illinois, USA) that maintains a temperature from − 25 to 100 *˚C*. For MFC experiments, *Shewanella oneidensis* MR-1 was cultivated from ATCC®, catalog № 700550™ (Virginia, USA) using tryptic soy broth at 30 *g/L* for 24 *h*. To avoid bacterial contamination the media and the solutions were sterilized using an autoclave at 121°C and 15 *psi*. The bacterial growth was evaluated using UV spectrophotometer at an optical density (OD) of 600 *nm*.

The samples collected during the experiments were analyzed for zinc concentrations using an inductively coupled plasma (ICP) instrument. The parameters of the feed solution, brine and melted iced (treated solution) were measured using water quality meters. The main instruments used to fulfil laboratory experiments are shown in Table 2.

Table 2
Main instruments used in the laboratory study

| Instrument | Accuracy | Supplier |
|---|---|---|
| Circulating chiller NESLAB RTE-7 | 0.1 *˚C* | Thermo Scientific (New Hampshire, USA) |
| Conductivity, salinity, and total dissolved solids meter | 1 *%* | OMEGA, (Connecticut, USA) |
| Data logger multimeter | 0.5 *%*±2 | Owon OW18 Series (Zhangzhou, China) |
| Digital thermometer with a temperature probe | 0.05 *˚C* | Traceable® (Texas, USA) |
| ICP | 0.01 *mg/L* | Bureau Veritas (Ontario, Canada) |
| Data acquisition software | N/A | Traceable® (Texas, USA) |
| Magnetic stirrer mixer | N/A | VWR (Alberta, Canada) |
| Electric overhead stirrer mixer | N/A | Vevor (California, USA) |
| Centrifuge | N/A | Thermo Scientific (USA) |
| N/A – not applicable | | |

# Laboratory setup and methods

# Cryopurification and data acquisition

Lab-scale cryopurification experiments were conducted using the set-up shown in Fig. 3a to examine the effects of ice front propagation, cooling temperature, and water mixing on zinc removal. Three cylindrical vessels were used in the experiments and ice shapes of different geometries were produced by each vessel. The vessel that produced glass-like ice shapes (Fig. 3b) was made from stainless-steel. Within this vessel, a freezing front spread from the stainless-steel walls and bottom. To eliminate heat flux through the bottom of vessel #2, which produced pipe-like shapes of ice (Fig. 3c), an additional layer of cork was added. In this vessel, a freezing front spread radially from the stainless-steel walls to the center. Vessel #3, a plastic cylinder with insulated walls and a bottom, produced a solid block of ice when freezing front propagated top-down (Fig. 3d). In most cases, laboratory experiments were done in triplicate.

In current study, the laboratory experiments procedure on cryopurification described by Popugaeva et al. 2023 was followed. Experiments were conducted in a cooling temperature range of − 15 to − 0.5 $^{\circ}C$. Within vessels #1 and #2, a rectangular agitator was used to investigate the effects of water mixing (180 rpm) on zinc removal from Faro Mine water. A magnetic stirrer was used for experiments with vessel #3. For a typical cryopurification experiment, 170 mL of Faro Mine water was filled into the vessel and a water sample was taken for zinc testing, temperature, salinity, and TDS testing. The initial temperature of Faro Mine water was maintained at 10 ± 1 $^{\circ}C$. The ice fraction (amount of water converted into ice during the experiments) of approximately 35% was used for each experiment, as an optimal ice fraction percentage for cryopurification experiments (Popugaeva et al. 2023).

Filled with feed water, vessels #1, and #2 were placed inside the chiller bath at a certain freezing temperature, one at a time. The water temperature was recorded throughout the experiment every 0.5 minutes using a temperature probe placed approximately 2.5 cm from the vessel wall. After ice formation reached a target thickness, the freezing process was stopped, and the brine solition was separated from the ice. For a set of experiments with vessel #3, a stainless-steel container with a circulating coolant medium was used as a cooling unit. Vessel #3 was filled with 170 *mL* of Faro Mine's water and a cooling unit was placed at the water surface. Both, the vessel, and cooling unit were insulated with polyurethane foam from the outside laboratory environment.

A sample of brine and melted ice was collected to record the measurements for temperature, salinity, and zinc and TDS concentration. By comparing zinc concentration in melted ice to the initial conditions, the purity of ice produced through cryopurification using vessels #1, #2, and #3 was quantified. Next step within the treatment process was the application of MFC – the produced brine was used as a feed solution for a set of laboratory experiments using MFC.

# Microbial fuel cell set-up and data acquisition

The MFC setup used in the experimental analysis is shown in Fig. 4. Dual-chamber MFC with a volume capacity of 500 *mL* for anode and cathode chamber was separated by an anion exchange membrane (AXM-100) based on gel polystyrene cross-linked with divinylbenzene with a thickness of 0.45 ± 0.025 *mm*, and an area of 36 $cm^2$ was purchased from the Membranes International Inc. (New Jersey, USA). An

external resistance of 1000 $\Omega$ connected the anode and cathode chambers. The goal of MFC experiments was to determine the residual zinc concentration after bacterium cultivation in the anode chamber generating power simultaneously.

The anode chamber was fed with the brine solution produced through cryopurification process and followed by the addition of tryptic soy broth (TSB) at 30 *g/L*, mineral solution (M9, a buffered minimal microbial medium) at 11.3 *g/L*, and sodium lactate 18 *mM*. The anode chamber was inoculated with *Shewanella oneidensis* at an optical density $OD_{600nm}$ of 0.53 ± 0.1. The temperature (*T*) was kept constant at 30°C using an incubator with mixing at 80 *rpm*. $K_3[Fe(CN)_6]$ at a concentration of 50 *mM* in phosphate buffer solution (PBS) 100 *mM* was as catholyte solution. The voltage output was displayed as response of the electron transport from anode to cathode chamber. The external resistance was changed from 10 to 80000 $\Omega$ to obtain the polarization curves. The voltage was measured with a multimeter with data logging. The data was stored every hour for 120 *h* with the addition of TSB and M9 to the anode chamber every 24 *h*. Watts's and Ohm's laws were used for the determination of current density (*I*) and power density (*P*) (Logan 2008).

# Evaluation of zinc removal efficiency

The effectiveness of cryopurification towards zinc removal from Faro mine water was quantitatively estimated using equations 1 and 2 2 (Miyawaki and Inakuma 2021; Moharramzadeh et al. 2021). The ice fraction was calculated using Eq. 3. A high-quality cryopurification process is achieved when the partition coefficient *K* value (Eq. 1) is close to zero and there is a high removal percentage (Eq. 2).

$$K = \raisebox{1ex}{\$}C_{ice}\$ \Big/ \raisebox{-1ex}{\$}C_{brine}\$ \quad (1)$$

$$Removal\,(\%) = (1 - \raisebox{1ex}{\$}C_{ice}\$ \Big/ \raisebox{-1ex}{\$}C_0\$\,) * 100 \quad (2)$$

$$Ice fraction\,(\%) = \raisebox{1ex}{\$}V_{ice}\$ \Big/ \raisebox{-1ex}{\$}V_0\$ * 100 \quad (3)$$

where, $C_{ice}$ – zinc concentration in melted ice (*mg/L*), $C_{brine}$ – zinc concentration in brine (*mg/L*), $C_0$ – initial zinc concentration in Faro mine water (*mg/L*), $V_{ice}$ – volume of melted ice (*mL*), $V_0$ – initial volume of Faro mine water (*mL*).

For MFC experiments, total zinc concentration was measured using ICP at three different times (0, 24, and 120 *h*) after centrifugation of the solution for bacteria separation. Centrifugation was done at 7000 *g*-force for 20 *min*, and the supernatant was sampled for zinc analysis. Moreover, for the evaluation of zinc uptake by the bacteria after 24 *h*, the solution was centrifuged with the same conditions. The supernatant was collected, and the bacteria cells were resuspended and washed with PBS solution three times. A sonicator was used for extracellular membrane breaking. The solution was centrifuged again with the

same conditions and the supernatant was then evaluated for total zinc. Analogously to Eq. 2, zinc removal through MFC was evaluated.

## Results and Discussion

# The effect of coolant temperature and ice shape

Ice purity is influenced by the cooling rate, which controls crystal growth. As the cooling rate increases, contaminant inclusions in the crystal layer may increase (Ila and Louhi-Kultanen 2023). The cooling rate can be controlled by freezing temperature, $T_f$. The effect of $T_f$ (−15 to − 0.5 $^{\circ}C$) on the purity of ice at a constant ice fraction (approximately 35%) was investigated in a set of laboratory experiments. According to the results of experiments, the purest ice was produced at the lowest cooling rate when $T_f$ was − 1 $^{\circ}C$ to − 0.5 $^{\circ}C$ (Fig. 5). The highest zinc removal up to 81% was achieved using vessel #3, while vessel #2 and vessel #1 showed 72% and 57% zinc removal, respectively, as the results of laboratory experiments revealed. Freezing from the top-down (vessel #3) facilitated better contaminant removal compared to vessels #1, and #2 which can be explained by a natural convection that was developed under the ice in vessel #3 leading to a better solution mixing and as a result, higher contaminant removal. A similar trend was observed in other study (Jayakody et al. 2017) concluding that freezing from the top-down was more efficient due to natural convection as compared to freezing from the bottom and lateral freezing.

Natural convection, laminar and turbulent mixing all could determine the conditions in which ice crystals nucleate and grow improving the effectiveness of cryopurification (Green 2019). Laboratory experiments on cryopurification could be fulfilled by using various solution movement mechanisms, including, but not limited to natural convection, stirring, circulation due to aeration, and ultrasonic radiation (Samsuri et al. 2016).

# The effect of a constant solution stirring

The effect of a constant 180 *rpm* mixing on zinc removal was investigated in the $T_f$ range of − 1 to − 15 $^{\circ}C$ and ice fraction of ≈ 35% by stirring a solution (Fig. 6). The results of the set of experiments revealed a significant increase in zinc removal under mixing reaching up to 92–95% removal. Removal of up to 35–52% using vessel #1 and vessel #2, respectively at lower $T_f$ was achieved. That was significantly higher compared to the experiments without mixing. The results obtained were consistent with previous literature findings (Moharramzadeh et al. 2021; Xu et al. 2022) concluding that stirring could significantly improve ice purity.

The tendency to obtain purer ice using freezing from the top-down freezing was consistent in experiments with and without mixing at $T_f$ from − 5 to − 15 $^{\circ}C$, as the results of data analysis revealed. The results showed that the removal rate in general followed the sequence of vessel #3 > vessel #2 > vessel #1, both with and without stirring (Table 3). Freezing from the top-down using vessel #3 enabled a convection movement leading to better solution mixing and therefore, higher zinc removal.

Table 3
The effects of solution stirring, freezing temperature, $T_f$ and ice shape on the efficiency of zinc removal based on the calculated partition coefficient, $K$

| $T_f$, ˚C | $K$, vessel #1 | | $K$, vessel #2 | | $K$, vessel #3 | |
|---|---|---|---|---|---|---|
| | No stirring | Stirring | No stirring | Stirring | No stirring | Stirring |
| −1 | 0.57 | 0.03 | 0.36 | 0.05 | 0.16 | 0.05 |
| −5 | 0.87 | 0.22 | 0.87 | 0.15 | 0.24 | 0.09 |
| −10 | 0.94 | 0.54 | 0.93 | 0.36 | 0.64 | 0.29 |
| −15 | 0.94 | 0.63 | 0.95 | 0.45 | 0.87 | 0.28 |

Initial zinc concentration, its concentrations in the melted ice and brine solutions were evaluated in each experiment. The distribution of zinc concentration in various fractions at $T_f$ − 15 ˚C is shown in Fig. 7. In comparison to zinc concentrations in raw feed water, melted ice contained 27–64% less zinc, while the concentration of zinc in brine increased by 15–32% depending on the vessel used in the experiment. The melted ice salinity could be decreased from 0.9 to 0.1 *ppt* while the brine salinity reached up to 1.2–1.3 *ppt*, as the results of experiments showed. A similar trend with TDS concentration was observed, TDS concentration decreased from 1.20 to 0.07 *g/L* in melted ice and increased to 1.6 *g/L* in brine reaching a removal up to 30–94%. The brine produced using vessel #2 and vessel #3 at $T_f$ of − 1 ˚C was used as feed water for MFC experiments with an average initial zinc concentration of 16.8 and 17.8 *mg/L*, respectively.

# Microbial fuel cell performance

Power density curve showed a maximum ($P_{max}$) peak at a current density of 63.8 $mA/m^2$ with a result of 8.80 $mW/m^2$ (Fig. 8). The optimal external resistance ($R_{ext}$) from the polarization curves was 800 $\Omega$, corresponding to the maximum power density produced at that external resistance. This was used as external resistance for the open-circuit voltage (OCV). Pmax for single-chamber MFCs with removal of cadmium and zinc was 3600 $mW/m^2$ (Abourached et al. 2014), and chromium, copper, and vanadium in a dual-chamber MFCs was 138.72 $mW/m^2$ (Aiyer 2020). Moreover, the use of acid mine drainage in MFCs showed a $P_{max}$ of 195.07 $mW/m^2$, 51.3 $mW/m^2$ (Peng et al. 2017), and 400 $mW/m^2$ (Stefanova et al. 2018). This study showed a power density that was lower in comparison with the results of another research. However, the power density is related to the size and distribution of the electrodes that in this case were not coated and the use of conventional copper wires decreased the rate of electron transport through the external circuit. Moreover, this maximum power density determined the internal resistance ($R_{int}$) because at the maximum point, $R_{ext} = R_{int}$. At this point, the less potential difference in the MFC made the electron transport more efficient.

Additionally, the polarization curve showed a maximum voltage of 292.3 *mV* (Fig. 8). The polarization curve demonstrates a slope of 1.9, the slope demonstrates the low internal resistance of this system and

the efficient electron transport. In addition, the polarization curve demonstrates a low loss of mass transfer polarization after 109.9 $mW/m^2$, indicating a better diffusion of the protons through the membrane. In comparison, a faster decrease in the same zone of mass transfer loss, which demonstrated a better efficiency in this system (Aiyer 2020). Similarly, the high mass transfer losses showed a fast reduction in electron transport, however, the use of goethite as an electrode showed a better performance in comparison to carbon felt used in this study (Jadhav et al. 2015). Additionally, a high temperature of 40°C showed a higher power density of 511 $mW/m^2$ (Stefanova et al. 2018).

Figure 9 shows four different peaks that were related to the feed in the anode chamber every 24 *h*. In addition, after 36 *h* the concentration losses in the OCV were higher, however due to the constant feeding the reduction was not as high as the control MFC, which was operated with TSB in the anode chamber. However, a higher OCV above 300 *mV* for zinc removal from wastewater in the cathode chamber was previously shown using MFC (Fradler et al. 2014; Lim et al. 2021). The lower OCV in this study could be a response of the toxicity of the wastewater in the bacteria metabolism which reduced the electron transport. The control media OCV was reduced due to the reduction in the redox potential during the operation because the electron donor was not sufficient for the oxidation process.

# The effect of microbial fuel cell in zinc removal

Zinc removal was measured at the beginning of the MFC operation, after 24 *h* and at 120 *h*, with a constant temperature of 30°C. The results are reported in Table 4. The experiments had different initial zinc concentrations corresponding to two brine solutions obtained at $T_f - 1\,^{\circ}C$ using vessel #2 and vessel #3 and raw feed water (before freezing). Initial zinc concentration influenced the removal efficiency showing a tendency for higher removal with high initial zinc concentration in MFC experiments (Table 4). The highest removal was 93*%* in 120 *h* at an initial zinc concentration of 17.8 *mg/L.* Based on the results of laboratory experiments on MFC, it was shown that the highest removal rate occurred in the first 24 *h* because the activity of the microorganism was higher due to their almost exponential growth phase for brine-concentrated water between 0 and 8 *h* (Fig. 10).

Table 4
Zinc removal by MFC with solution fed in the anode chamber

| **Time, *h*** | **Experiment I (Brine)** | | **Experiment II (Brine)** | | **Experiment III (Raw feed water)** | |
|---|---|---|---|---|---|---|
| | **Concentration, *mg/L*** | **Removal, *%*** | **Concentration, *mg/L*** | **Removal, *%*** | **Concentration, *mg/L*** | **Removal, *%*** |
| 0 | 17.8 | N/A | 16.8 | N/A | 13.7 | N/A |
| 24 | 2.4 | 87 | 2.3 | 86 | 3.0 | 78 |
| 120 | 1.2 | 93 | 1.4 | 92 | 1.4 | 90 |
| N/A – not applicable | | | | | | |

The initial concentration of brine water was 17.8 *mg/L* and 16.8 *mg/L*, and 13.7 *mg/L* for raw feed water. The results showed that in the first 24 *h* the bacterium in the almost exponential phase has a higher metal absorption with values of 87*%*, 86*%*, and 78*%* for experiments I, II and III, respectively. Similarly, cadmium and lead absorption from wastewater were 64% and 51%, respectively (Raghad et al. 2016). Additionally, biofilm on zeolite of different bacteria such as *Shewanella xiamenensis* with zinc biosorption of 78*%* (Zinicovscaia et al. 2020), and 74*%* (Zinicovscaia et al. 2021). However, the bacterium growth with brine concentrated showed a low rate in comparison with TSB. The TSB was the optimum bacterium media for growth allowing a better nutrient uptake, which enhances the bacterial growth rate. Additionally, high concentrated heavy metals increase the toxicity inhibiting the growth of the bacterium. *Shewanella oneidensis* uses the cytochromes CymA and MtrCAB complex in the extracellular membrane and bacterial nanowires. In addition, MTrC and OmcA cytochromes are terminal reductases for the metal ions (Yin et al. 2022). These cytochromes are multi-heme proteins with high redox activity that facilitated the EET and metal respiratory pathway (Otero et al. 2020). Moreover, the higher absorption of the bacteria in the first 24 *h* helped in the formation of extracellular proteins (Ge et al. 2022). In addition, *S. oneidensis* growth with brine concentrated by freezing presented an absorption of 15.9 *mg/L* during the first 24 *h*. This was analyzed using a cultivation of the bacterium in a media with the zinc at initial concentration of 16.9 *mg/L*. However, the higher metal absorption showed a lower bacterial growth in comparison with the growth with tryptic soy broth.

## Conclusions

The proposed approach including cryopurification followed by MFC for post-cryopurification brine treatment could be an environment-friendly approach for treating highly contaminated Faro Mine's water in the Yukon Territory, Canada. Based on the results of the current study, zinc concentrations could be reduced close to the effluent quality criteria of 0.5 *mg/L* providing a removal of up to 90–95*%* under optimal laboratory conditions. In addition to zinc removal, the approach showed the possibility of power generation using MFC process. One of the important parts of the proposed treatment approach is that no chemicals were used to purify the water. Water ecosystems of northern environments are fragile and if damaged, a long recovery is expected. This, along with the Yukon's cold climate conditions enhancing the efficiency of cryopurification application and the local availability of bacterial cultures for metal remediation, could make applying the proposed and tested green approach to the Faro Mine site more sustainable and save energy.

## Declarations

# Acknowledgments

The financial support for this research work was provided by Natural Sciences and Engineering Council of Canada (NSERC) along with MITACS and Core Geoscience Services Inc. (CoreGeo) under the NSERC MITACS Alliance grant (Project Grant No. R3839A47). We would like to acknowledge CoreGeo for

providing us with the Faro Mine's water samples and for their constant support and discussions that facilitated this research work.

# References

1. Abourached C, Catal T, Liu H (2014) Efficacy of single-chamber microbial fuel cells for removal of cadmium and zinc with simultaneous electricity production. Water Res 51:228–233. https://doi.org/10.1016/j.watres.2013.10.062
2. Ai C, Yan Z, Hou S, et al (2020) Effective treatment of acid mine drainage with microbial fuel cells: An emphasis on typical energy substrates. Minerals 10:. https://doi.org/10.3390/min10050443
3. Aiyer KS (2020) Recovery of chromium, copper and vanadium combined with electricity generation in two-chambered microbial fuel cells. FEMS Microbiol Lett 367:. https://doi.org/10.1093/femsle/fnaa129
4. Alexandre LHZ, Pineda-Vásquez TG, Watzko ES, et al (2022) An Evaluation of the Potential Use of Microbial Fuel Cells for Energy Production and Simultaneous Acid Mine Drainage Treatment. Water Air Soil Pollut 233
5. Crown-Indigenous Relations and Northern Affairs Canada (2021) Faro Mine Remediation Project: Yukon. https://www.rcaanc-cirnac.gc.ca/eng/1480019546952/1537554989037. Accessed 1 December 2023
6. Dixit R, Wasiullah, Malaviya D, et al (2015) Bioremediation of Heavy Metals from Soil and Aquatic Environment: An Overview of Principles and Criteria of Fundamental Processes. Sustainability 7:2189–2212. https://doi.org/10.3390/su7022189
7. Dutta K, Kundu PP (2018) Introduction to microbial fuel cells. In: Progress and Recent Trends in Microbial Fuel Cells. Elsevier, pp 1–6
8. Fradler KR, Michie I, Dinsdale RM, et al (2014) Augmenting microbial fuel cell power by coupling with supported liquid membrane permeation for zinc recovery. Water Res 55:115–125. https://doi.org/10.1016/j.watres.2014.02.026
9. Gadd MG, Layton-Matthews D, Peter JM, et al (2017) The world-class Howard's Pass SEDEX Zn-Pb district, Selwyn Basin, Yukon. Part II: the roles of thermochemical and bacterial sulfate reduction in metal fixation. Miner Depos 52:405–419. https://doi.org/10.1007/s00126-016-0672-x
10. Ge C, Huang M, Huang D, et al (2022) Effect of metal cations on antimicrobial activity and compartmentalization of silver in Shewanella oneidensis MR-1 upon exposure to silver ions. Science of The Total Environment 838:156401. https://doi.org/10.1016/j.scitotenv.2022.156401
11. Green DA (2019) Crystallizer mixing: Understanding and modeling crystallizer mixing and suspension flow. In: Handbook of Industrial Crystallization. Cambridge University Press, pp 290–312
12. Hasan M, Louhi-Kultanen M (2016) Water purification of aqueous nickel sulfate solutions by air cooled natural freezing. Chemical Engineering Journal 294:176–184. https://doi.org/10.1016/j.cej.2016.02.114

13. Ila M, Louhi-Kultanen M (2023) Purification of monoethylene glycol by melt crystallization. Chem Eng Sci 272:118601. https://doi.org/10.1016/j.ces.2023.118601
14. Jadhav DA, Ghadge AN, Ghangrekar MM (2015) Enhancing the power generation in microbial fuel cells with effective utilization of goethite recovered from mining mud as anodic catalyst. Bioresour Technol 191:110–116. https://doi.org/10.1016/j.biortech.2015.04.109
15. Jayakody H, Al-Dadah R, Mahmoud S (2017) Computational fluid dynamics investigation on indirect contact freeze desalination. Desalination 420:21–33. https://doi.org/10.1016/j.desal.2017.06.023
16. Lim SS, Fontmorin JM, Pham HT, et al (2021) Zinc removal and recovery from industrial wastewater with a microbial fuel cell: Experimental investigation and theoretical prediction. Science of the Total Environment 776:. https://doi.org/10.1016/j.scitotenv.2021.145934
17. Logan BE (2008) Microbial Fuel Cells, Wiley-Inte. John Wiley and Sons Inc., New Jersey
18. Makhalanyane TP, Van Goethem MW, Cowan DA (2016) Microbial diversity and functional capacity in polar soils. Curr Opin Biotechnol 38:159–166. https://doi.org/10.1016/j.copbio.2016.01.011
19. Melak F, Du Laing G, Ambelu A, Alemayehu E (2016) Application of freeze desalination for chromium (VI) removal from water. Desalination 377:23–27. https://doi.org/https://doi.org/10.1016/j.desal.2015.09.003
20. Min D, Cheng L, Zhang F, et al (2017) Enhancing Extracellular Electron Transfer of Shewanella oneidensis MR-1 through Coupling Improved Flavin Synthesis and Metal-Reducing Conduit for Pollutant Degradation. Environ Sci Technol 51:5082–5089. https://doi.org/10.1021/acs.est.6b04640
21. Miyawaki O, Inakuma T (2021) Development of progressive freeze concentration and its application: a review. Food Bioproc Tech 14:39–51. https://doi.org/10.1007/s11947-020-02517-7
22. Moharramzadeh S, Ong SK, Alleman J, Cetin KS (2021) Parametric study of the progressive freeze concentration for desalination. Desalination 510:. https://doi.org/10.1016/j.desal.2021.115077
23. Munoz-Cupa C, Hu Y, Xu C, Bassi A (2021) An overview of microbial fuel cell usage in wastewater treatment, resource recovery and energy production. Science of the Total Environment 754:142429. https://doi.org/10.1016/j.scitotenv.2020.142429
24. Najim A (2022) A review of advances in freeze desalination and future prospects. NPJ Clean Water 5
25. Najim A, Krishnan S (2023) Experimental study on progressive freeze-concentration based desalination employing a rectangular channel crystallizer. Environ Sci (Camb) 9:850–860. https://doi.org/10.1039/d2ew00892k
26. Najim A, Krishnan S (2022) Experimental and theoretical investigation of a novel system for progressive freeze-concentration based desalination process. Chemical Engineering and Processing - Process Intensification 173:. https://doi.org/10.1016/j.cep.2022.108821
27. Ni G, Christel S, Roman P, et al (2016) Electricity generation from an inorganic sulfur compound containing mining wastewater by acidophilic microorganisms. Res Microbiol 167:568–575. https://doi.org/10.1016/j.resmic.2016.04.010

28. Nielsen G, Coudert L, Janin A, et al (2019) Influence of Organic Carbon Sources on Metal Removal from Mine Impacted Water Using Sulfate-Reducing Bacteria Bioreactors in Cold Climates. Mine Water Environ 38:104–118. https://doi.org/10.1007/s10230-018-00580-3
29. Obileke KC, Onyeaka H, Meyer EL, Nwokolo N (2021) Microbial fuel cells, a renewable energy technology for bio-electricity generation: A mini-review. Electrochem commun 125:107003. https://doi.org/10.1016/J.ELECOM.2021.107003
30. Otero FJ, Yates MD, Tender LM (2020) Extracellular Electron Transport in Geobacter and Shewanella: A Comparative Description. In: Microbial Electrochemical Technologies. pp 3–14
31. Peng X, Tang T, Zhu X, et al (2017) Remediation of acid mine drainage using microbial fuel cell based on sludge anaerobic fermentation. Environmental Technology (United Kingdom) 38:2400–2409. https://doi.org/10.1080/09593330.2016.1262462
32. Popugaeva D, Allen E, Corriveau M, et al (2023) The application of freezing technology for zinc removal from Faro pit mine-impacted water, Yukon, Canada. Cold Reg Sci Technol 103922. https://doi.org/10.1016/j.coldregions.2023.103922
33. Popugaeva D, Allen E, Corriveau M, Govindaraj S (2021) Purification of mine-impacted water by freezing: laboratory data analysis and mathematical modeling. In: IWA Young Water Professionals Canadian National Conference
34. Raghad J, Amin AS, Asaad AT (2016) Bioaccumulation of cadmium and lead by Shewanella oneidensis isolated from soil in Basra governorate, Iraq. Afr J Microbiol Res 10:370–375. https://doi.org/10.5897/ajmr2016.7912
35. Samsuri S, Amran NA, Yahya N, Jusoh M (2016) Review on Progressive Freeze Concentration Designs. Chem Eng Commun 203:345–363
36. Shonet RDC (1987) The freeze desalination of mine waters
37. Stefanova A, Angelov A, Bratkova S, et al (2018) Influence of electrical conductivity and temperature in a microbial fuel cell for treatment of mining waste water. In: Annals of “Constantin Brancusi” University of Targu Jiu, Engineering Series. pp 18–24
38. Sulonen MLK, Kokko ME, Lakaniemi AM, Puhakka JA (2014) Electricity generation from tetrathionate in microbial fuel cells by acidophiles. J Hazard Mater 284:182–189. https://doi.org/10.1016/j.jhazmat.2014.10.045
39. The Government of Canada (2022) Metal Mining Effluent Regulations
40. Tongshuai L, Yan Z, Yuanqing T, et al (2022) Application of progressive freeze concentration in the removal of Ca2+ from wastewater. Journal of Water Process Engineering 46:. https://doi.org/10.1016/j.jwpe.2022.102619
41. Vélez-Pérez LS, Ramirez-Nava J, Hernández-Flores G, et al (2020) Industrial acid mine drainage and municipal wastewater co-treatment by dual-chamber microbial fuel cells. Int J Hydrogen Energy 45:13757–13766. https://doi.org/10.1016/j.ijhydene.2019.12.037
42. Wang X, Li J, Wang Z, et al (2016) Increasing the recovery of heavy metal ions using two microbial fuel cells operating in parallel with no power output. Environmental Science and Pollution Research

23:20368–20377. https://doi.org/10.1007/s11356-016-7045-y

43. Wijewardena D (2018) Toxic and precious metals removal from wastewater using freeze concentration and electrodeionization. Lakehead University
44. Xie GR, Choi CS, Lim BS, Chu SX (2020) Continuous removal of heavy metals by coupling a microbial fuel cell and a microbial electrolytic cell. Membrane and Water Treatment 11:283–294. https://doi.org/10.12989/mwt.2020.11.4.283
45. Xu C, Kolliopoulos G, Papangelakis VG (2022) Industrial water recovery via layer freeze concentration. Sep Purif Technol 292:. https://doi.org/10.1016/j.seppur.2022.121029
46. Yin Y, Liu C, Zhao G, Chen Y (2022) Versatile mechanisms and enhanced strategies of pollutants removal mediated by Shewanella oneidensis: A review. J Hazard Mater 440:129703. https://doi.org/10.1016/j.jhazmat.2022.129703
47. Yin Y, Yang Y, de Lourdes Mendoza M, et al (2017) Progressive freezing and suspension crystallization methods for tetrahydrofuran recovery from Grignard reagent wastewater. J Clean Prod 144:180–186. https://doi.org/10.1016/j.jclepro.2017.01.012
48. Youssef PG, Al-Dadah RK, Mahmoud SM (2014) Comparative analysis of desalination technologies. In: Energy Procedia. Elsevier Ltd, pp 2604–2607
49. Zinicovscaia I, Safonov A, Boldyrev K, et al (2020) Selective metal removal from chromium-containing synthetic effluents using Shewanella xiamenensis biofilm supported on zeolite. Environmental Science and Pollution Research 27:10495–10505. https://doi.org/10.1007/s11356-020-07690-y
50. Zinicovscaia I, Yushin N, Grozdov D, et al (2021) Zinc-containing effluent treatment using Shewanella xiamenensis biofilm formed on zeolite. Materials 14:. https://doi.org/10.3390/ma14071760

# Figures


**Figure 1**

The location of Faro Mine Complex (Yukon, Canada)

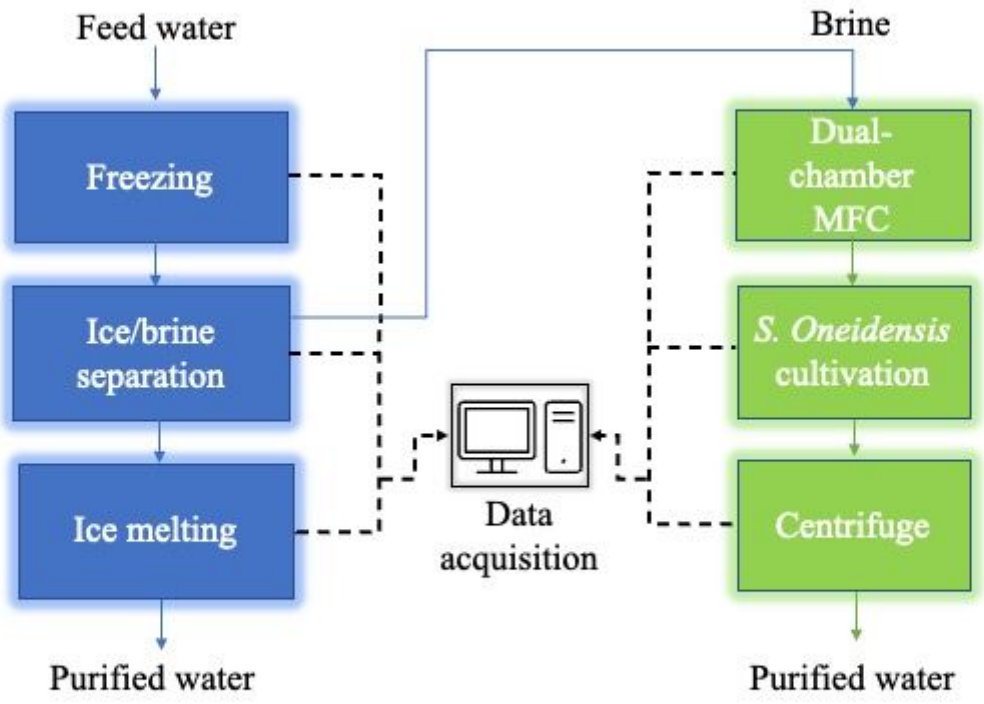


## Figure 2

Schematic design diagram of two main blocks of laboratory setup

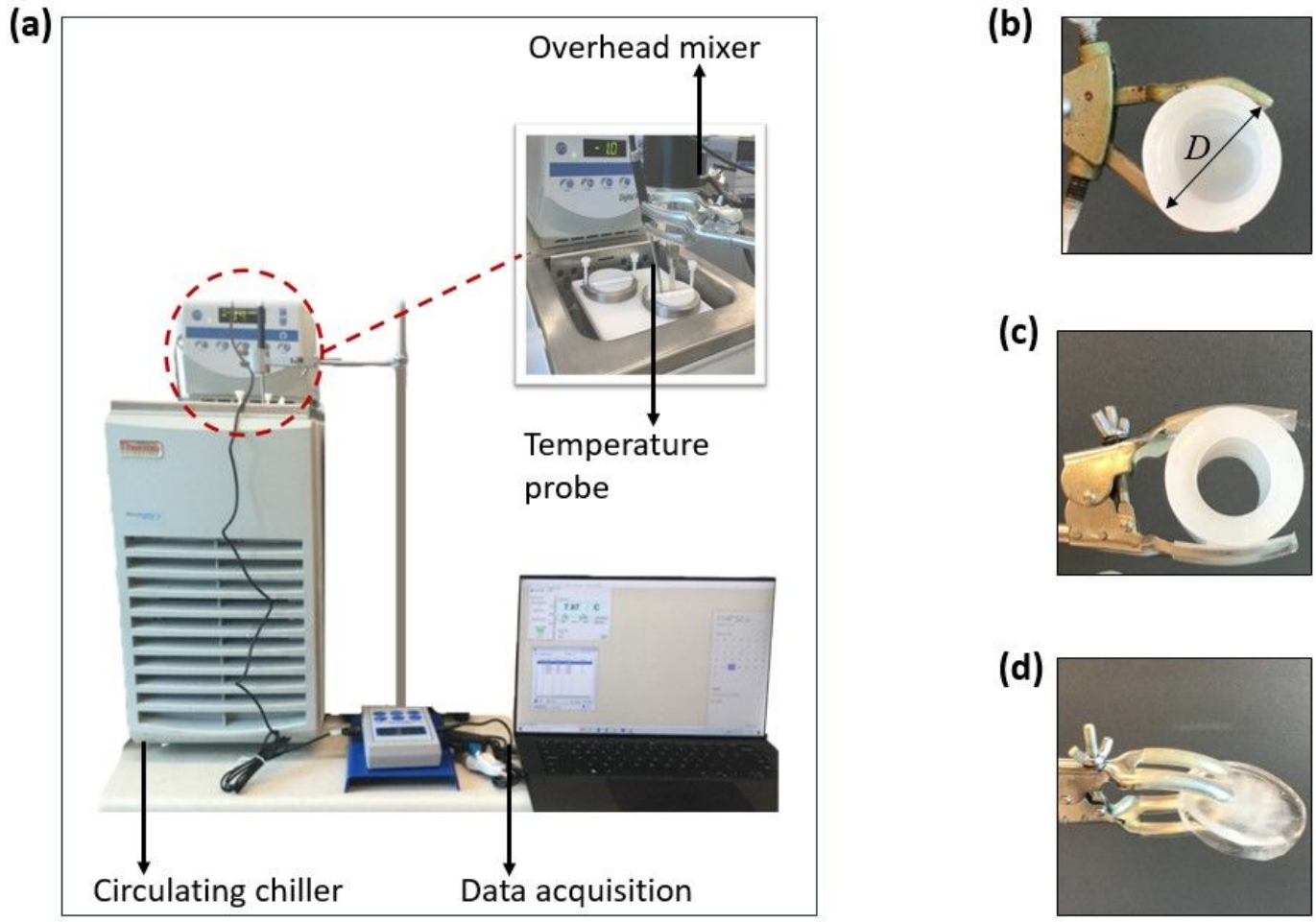


## Figure 3

(a) laboratory setup and various ice shapes samples produced depending on ice front propagation, (b) freezing from the walls and bottom using vessel #1, (c) freezing from the walls only using vessel #2, and (d) freezing from the top-down using vessel #3. The vessels (ice blocks) diameter, $D = 5.25\ cm$

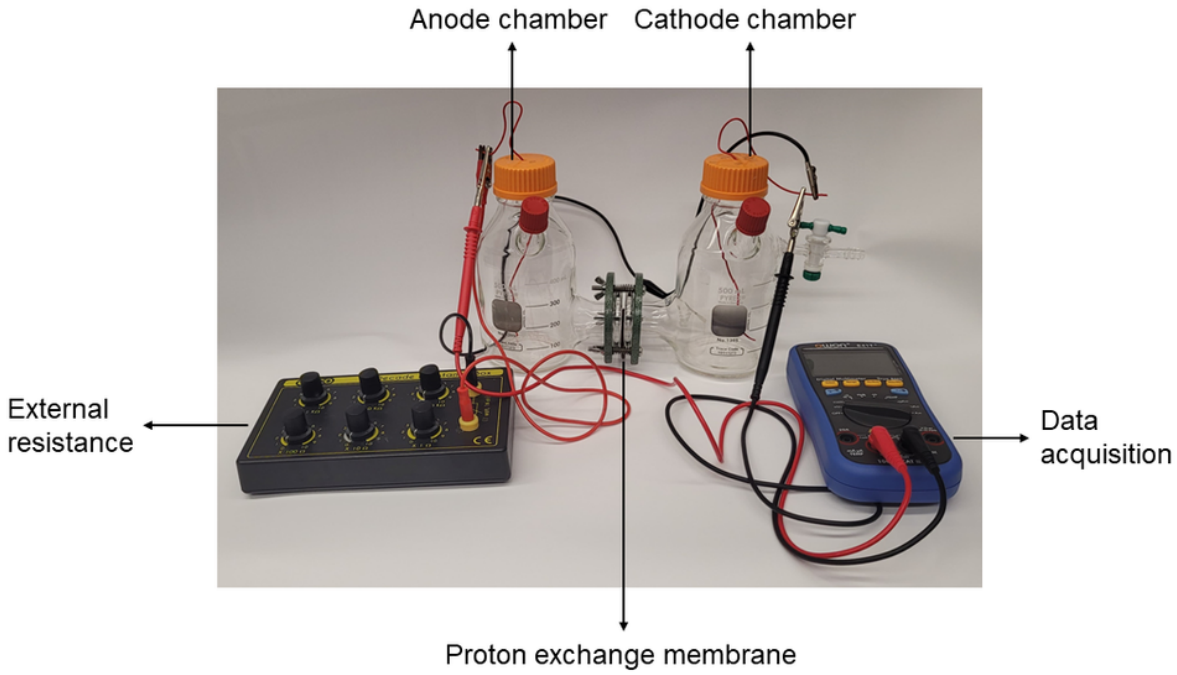


**Figure 4**

Dual-chamber microbial fuel cell set-up connected through and external resistance and a multimeter

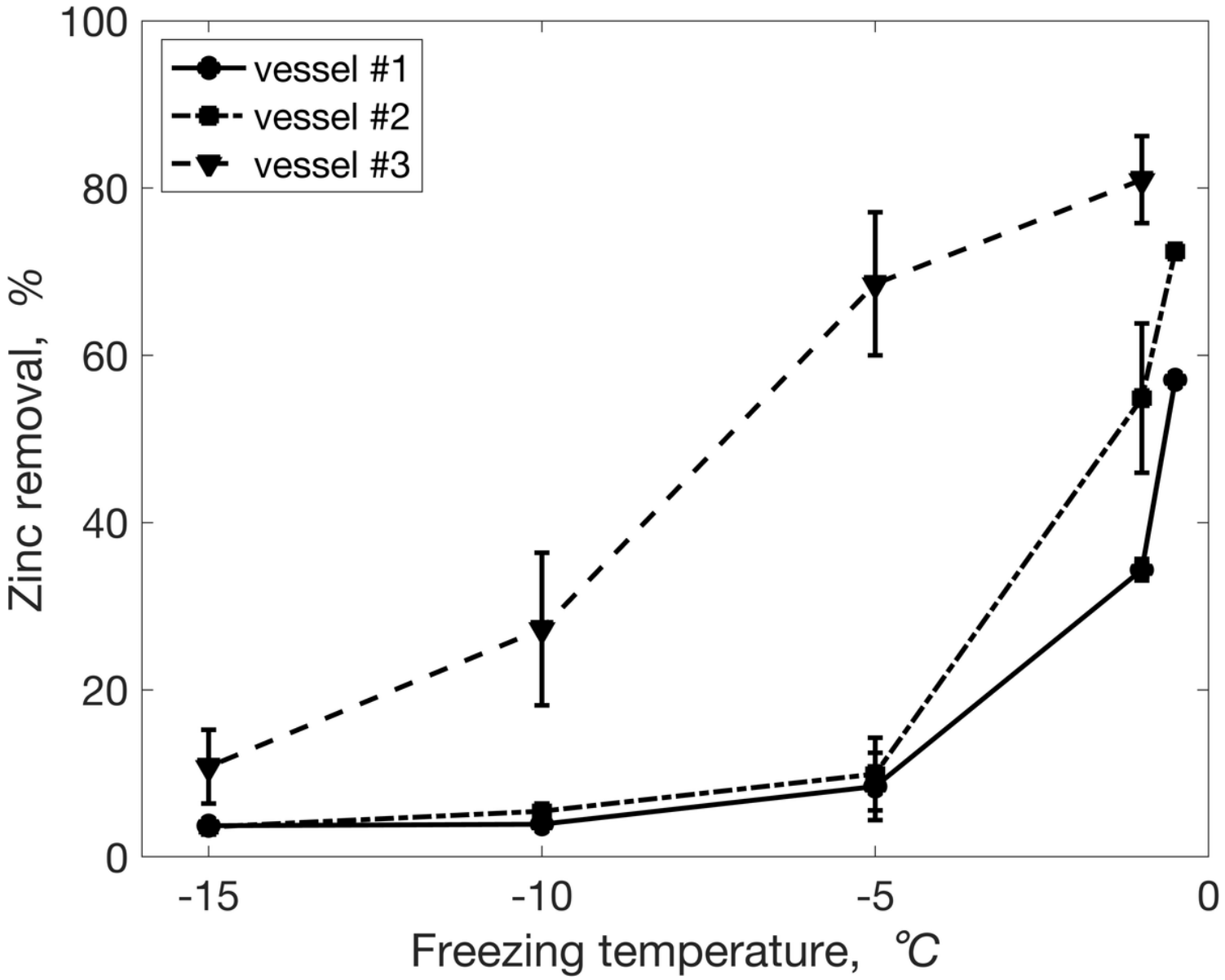


**Figure 5**

The effect of freezing temperature ($T_f$) on the purity of ice at constant ice fraction (≈ 35%) using laboratory vessels

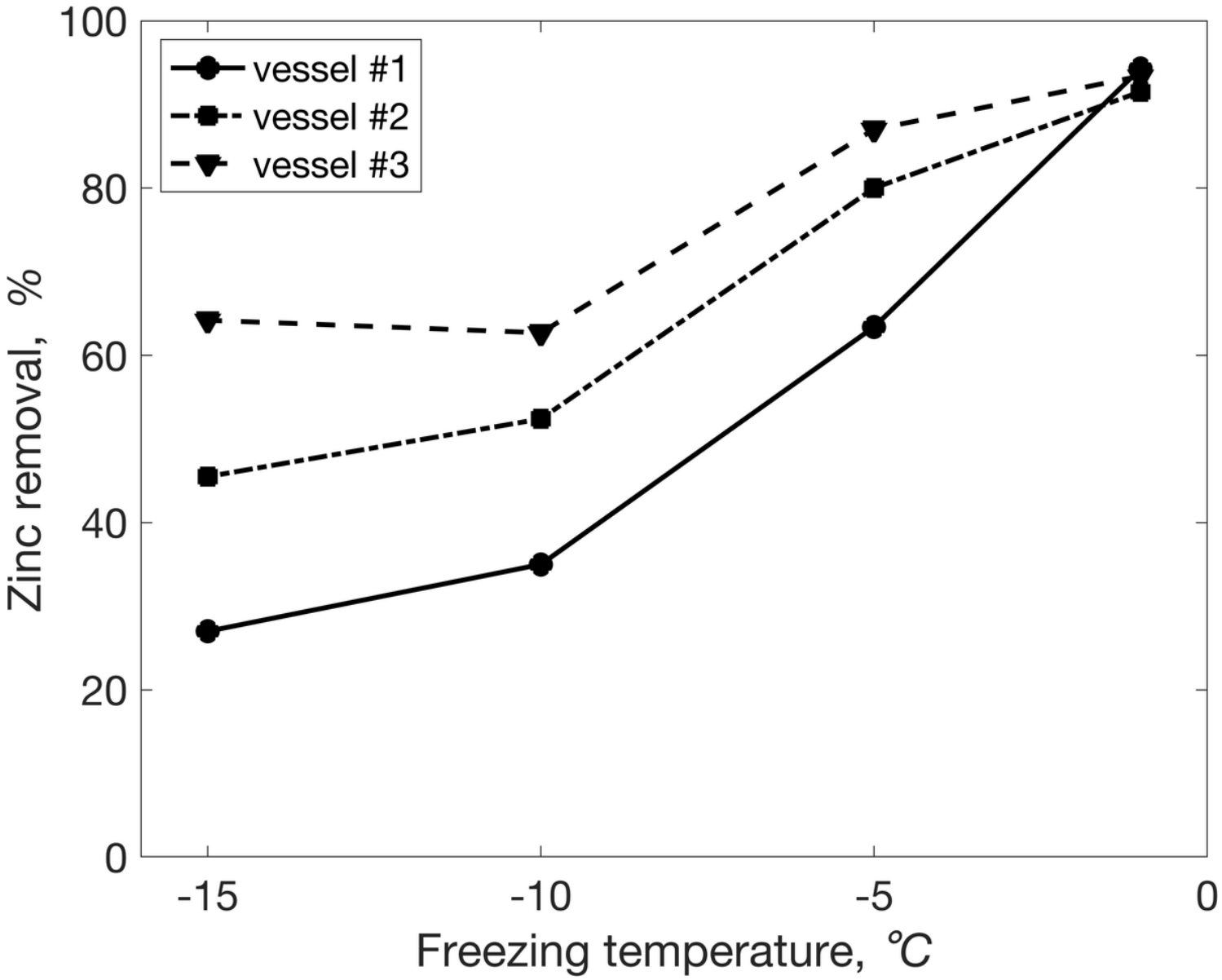


**Figure 6**

The effect of solution stirring on zinc removal. Experimental conditions: stirring speed 180 *rpm*, $T_f$ range −1 to −15 °*C*, ice fraction ≈ 35%

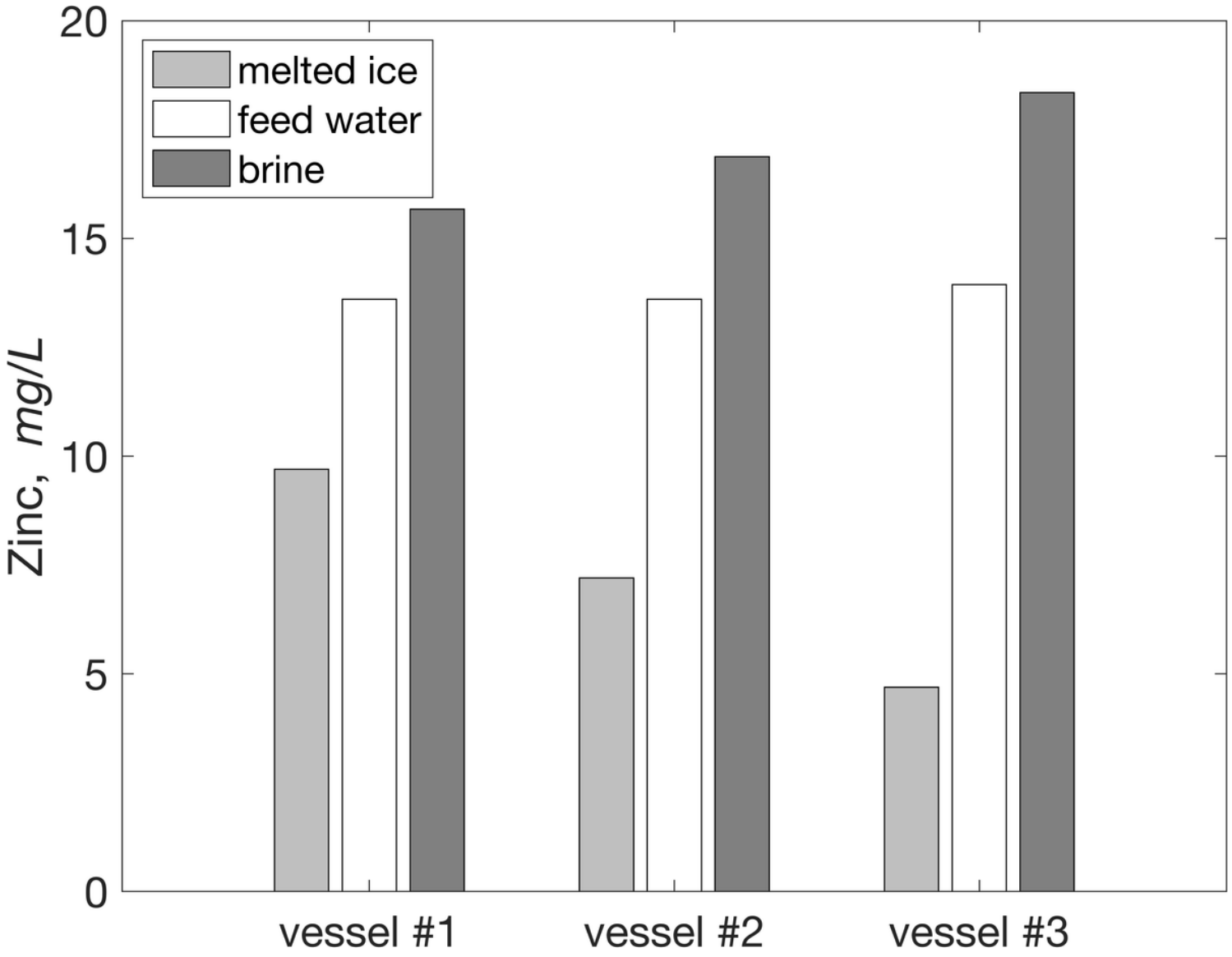


**Figure 7**

Zinc concentration in feed water, melted ice and brine. Experimental conditions: $T_f$ −15 $^{\circ}C$, ice fraction ≈ 35%, mixing speed 180 *rpm*

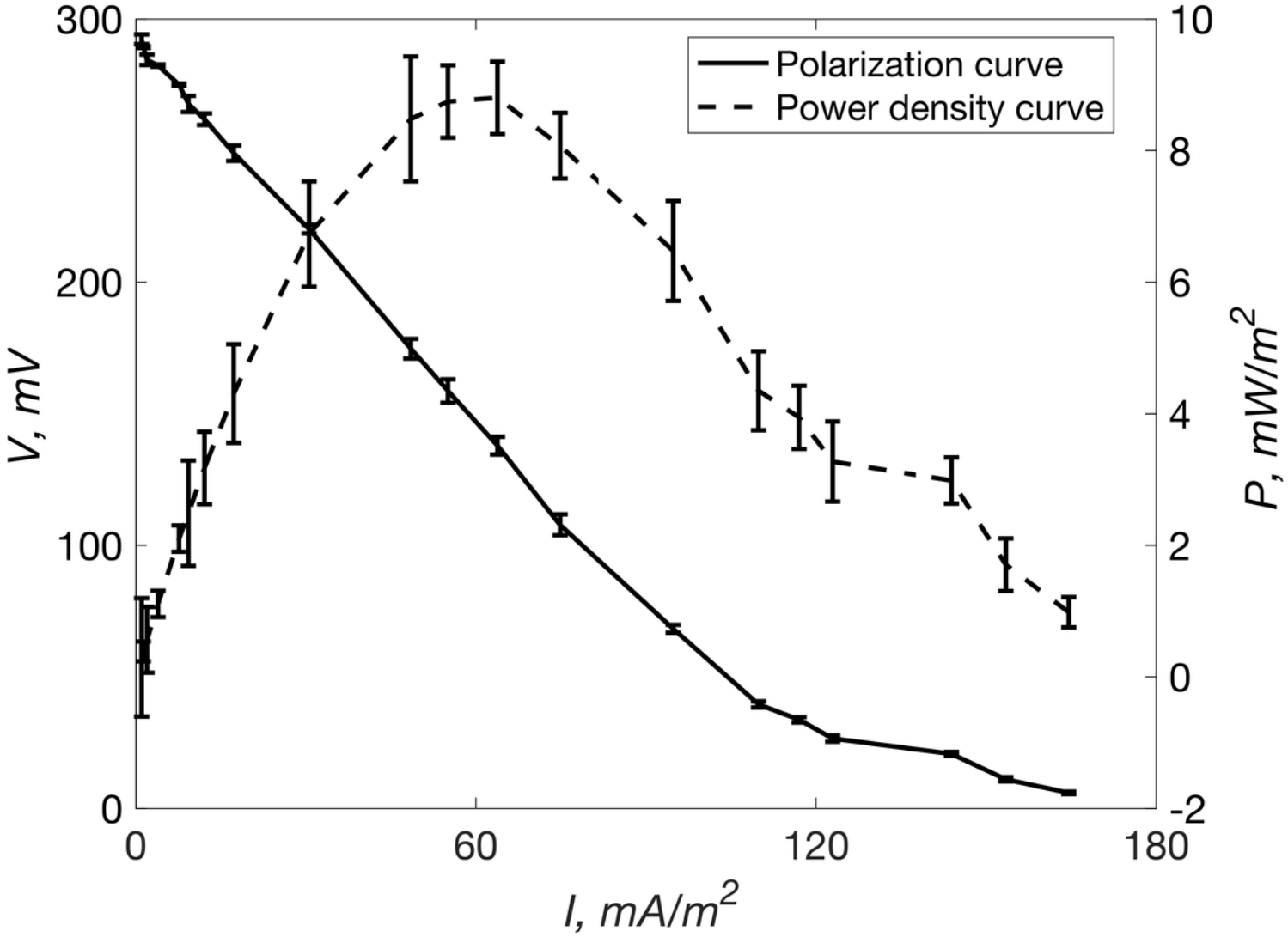


**Figure 8**

Polarization and power density curve evaluated varying the external resistance from 10 to 80000 $\Omega$ using a dual-chamber MFC

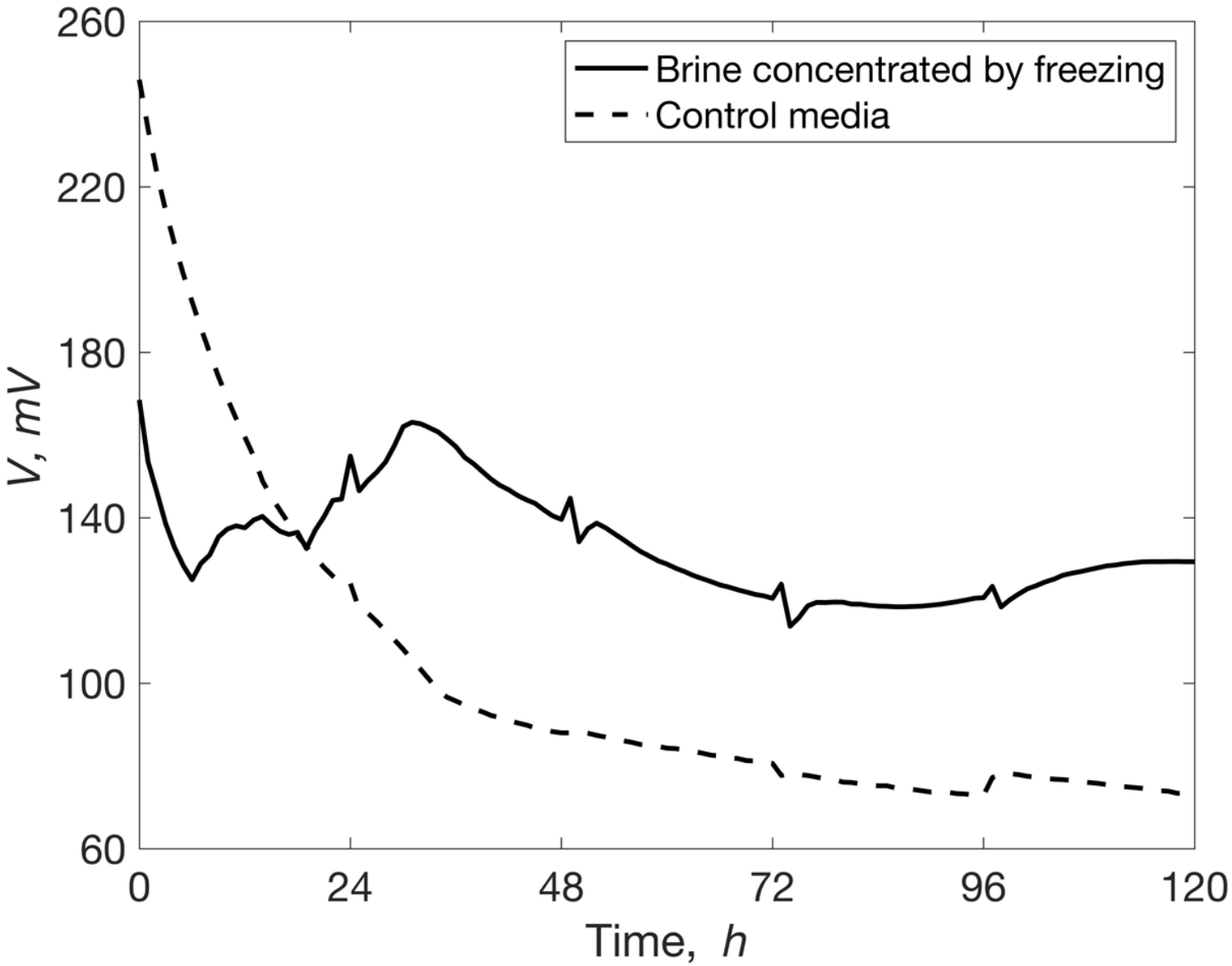


**Figure 9**

Open-circuit voltage evaluated for 120 *h* with anode feeding every 24 *h*. Experimental conditions: $T$ = 30 $^{\circ}C$, incubator mixing 80 *rpm*

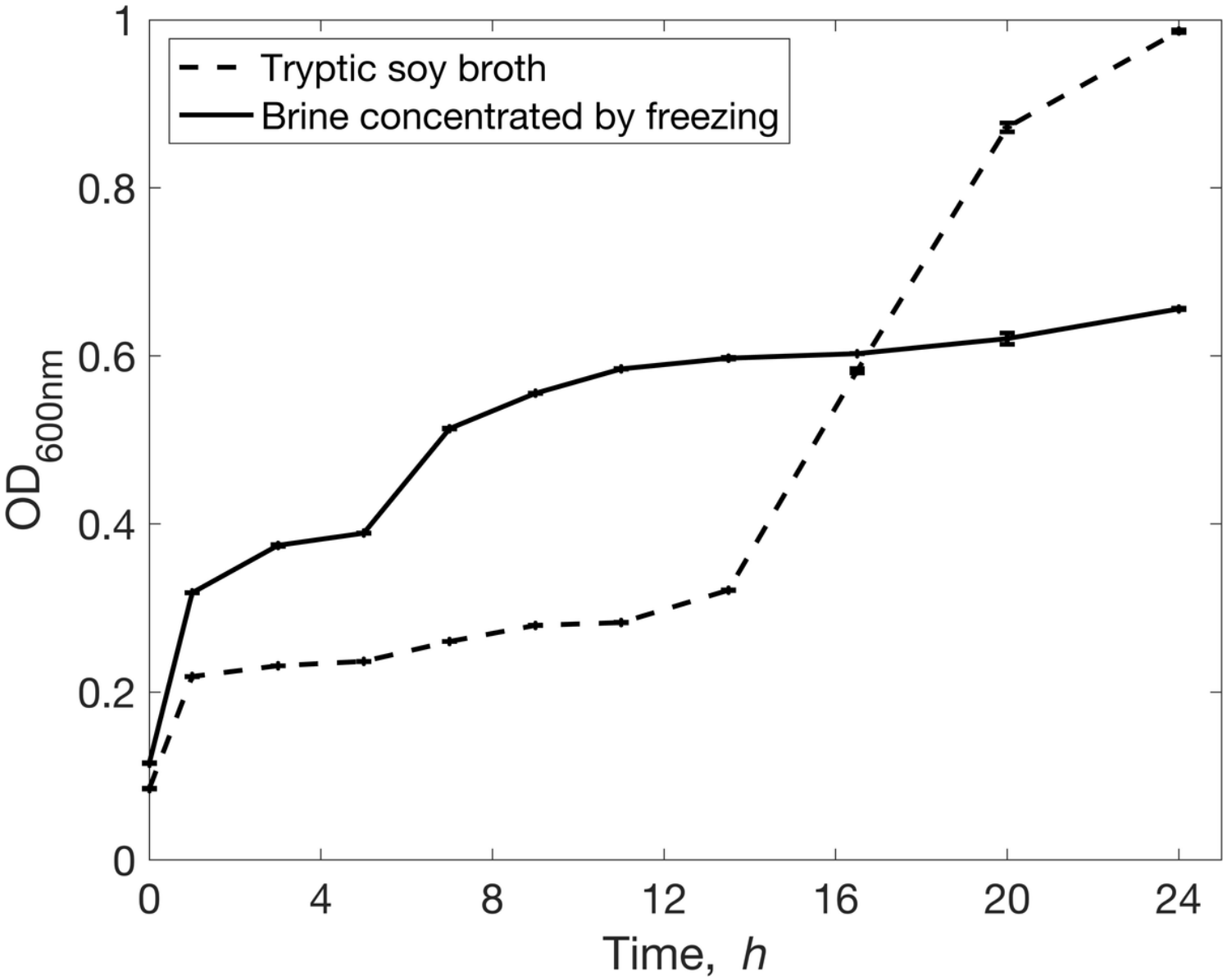


**Figure 10**

*Shewanella oneidensis* growth in brine concentrated by freezing with tryptic soy broth and zinc during the first 24 *h* of operation. Experimental conditions: $T$ = 30 *°C*